Gas sparger orifice sizes and solid particle characteristics in a bubble column - Relative effect on hydrodynamics and mass transfer

Kritchart Wongwailikhit, Passaworn Warunyuwong, Nattawin Chawaloesphonsiya, Nicolas Dietrich, Gilles Hébrard, Pisut Painmanakul

Gas sparger orifice sizes and solid particle characteristics in a bubble column - Relative effect on hydrodynamics and mass transfer

Kritchart Wongwailikhit[1,4], Passaworn Warunyuwong[1], Nattawin Chawaloesphonsiya[2,3], Nicolas Dietrich[4], Gilles Hébrard[4] and Pisut Painmanakul[1,3,a]

[1] Department of Environmental Engineering, Faculty of Engineering, Chulalongkorn University, Bangkok, Thailand 10330
[2] International Postgraduate Program in Environmental Management, Graduate School, Chulalongkorn University, Bangkok, Thailand
[3] Center of Excellence on Hazardous Substance Management (HSM), Chulalongkorn University, Thailand
[4] INSA, UPS, INPT; LISBP, Université de Toulouse, Toulouse, France
E-mail: [a]pisut.p@chula.ac.th

Abstract. The knowledge regarding the relative effect between the orifice size of gas sparger and solid particle properties on gas–liquid mass transfer have not yet been concerned. In this work, the effect of sparger orifice sizes, solid particle shapes and their loading amounts in a bubble column reactor for the absorption of oxygen in tap water were investigated. Their influences on the mass transfer coefficient and bubble hydrodynamic parameters were determined. The results showed that the addition of solid particles could have both positive and negative effects on the hydrodynamic and mass transfer depending on the orifice size of gas sparger. The negative effect was observed when the small orifice sparger (median diameter 0.15 mm) was used whilst the positive effect was obtained when the large orifice sparger (median diameter 0.75 mm) was applied. Different types and shapes of solid particles were tested. The ring-shaped particle was the optimal one providing the highest specific interfacial area and overall volumetric mass transfer coefficient as bubbles spent more time in the column resulting in longer contact time for the gas transfer. The introduction of solid particles can be suitable to improve the mass transfer performance in a bubble column without spending highly additional power consumption.

Keywords: Bubble column; Solid particles; Shape; Hydrodynamic; Mass transfer

1. INTRODUCTION

Gas absorption is a process of gas transfer into a liquid through the gas-liquid interface. This operation can be applied in many processes, for example, oxygenation in aerobic wastewater treatment or carbon dioxide absorption for biogas purification. Generally, a bubble column reactor is used for the gas absorption because of its advantages of low operating and maintenance costs, compactness, and high mass transfer rate [1].

However, the absorption rate can be improved through a modification of the bubble hydrodynamic, since it plays an important role in the bubble column. Several research works have attempted to enhance the absorption rate by increasing the interfacial area between the gas and liquid phases. The addition of surfactant in the liquid phase is one alternative for increasing the gas-liquid interfacial area by decreasing the bubble diameter [2,3]. However, the presence of surfactants can also decrease the liquid side mass transfer coefficient (k_L) [3,4]. Luo et al. [5] and Hébrard et al. [6] investigated the effects of the sparger structure on the hydrodynamics and mass transfer characteristics. It was found that the sparger with small orifice diameters and a large number of orifices provided a high mass transfer rate but the corresponding power consumption was increased.

Another approach is to apply solid phase in the bubble column. There were various works applying the packing bed into the bubble column. Moustiri et al. [7] studied the effects of static solid packing solid on the hydrodynamics of bubbles and found that the size and terminal rising velocity of the bubbles were reduced when static solid particles were present in the column. Bhatia et al. [8] also suggested that the specific interfacial area increased with solid. Maldonado et al. [9] indicated that the solid characteristics of a fixed bed bubble column could influence the mass transfer coefficient (k_La) as the decrease of particle size and bed porosity resulted in the reduction of the k_La.

Besides the static solid phase, several works also applied movable solids into their bubble columns but there were discrepancies observed from their works. Ferreira et al. [10] and Mena et al [11] applied different solid particles in bubble column and mostly found the negative effect on the k_La; whereas, Chandraserkaran et al. [12], Sada et al. [13] and Quicker et al [14] observed a positive effect on their k_La. The differences between physical properties of solid particles such as size, density, and loading were suggested to be responsible for these differences. Various works had been done investigated the effect of solid size, density and loading rate on the k_La [15–17]. However, none of them had investigated the effect of orifice size as well as the particle shape on the hydrodynamic and mass transfer in a bubble column with the presenting of movable solids.

Therefore, the objective of this study was to determine the relative effect orifice sparger size and particles properties. Two sizes of rigid spargers and four types of moveable solid particles were investigated their effect on both the hydrodynamics and mass transfer in a bubble column. Firstly, two different orifice size spargers were studied their effects without presenting of solids. Finally, small and large orifice spargers were compared and studied with the various solid particles to provide a better understanding and the role of solid particles in the absorption process. It was expected that the presenting of solids would rise the k_La without additional power consumption leading to better adsorption rate with lower operating cost.

2. MATERIALS AND METHODS

2.1 The Experimental Setup

2.1.1 Bubble Column

The experimental setup used in this study is schematically depicted in Figure 1. The experiments were carried out in a cylindrical acrylic column 0.14 m in diameter and 1 m in height. The column was filled with 10 L of tap water. A porous sparger was installed at the bottom of the column. Different sizes of porous spargers were used to determine the effects of orifice sizes on hydrodynamic and mass transfer. The small orifice and large orifice spargers consisted of various pores with diameter

ranges between 0.1 – 0.2 mm and 0.5 – 1.0 mm respectively. An HP-12000 air compressor was used to generate the gas phase injected through the sparger. Gas flow rates (Q_g) from 2.5 to 12.5 LPM were studied. This range corresponds to superficial gas velocities of $0.27x10^{-2}$ – $1.3x10^{-2}$ m/s; the gas flow rate was adjusted by a Dwyer gas flow regulator and its pressure was measured with a pressure gauge range between 0 to 1 barg.

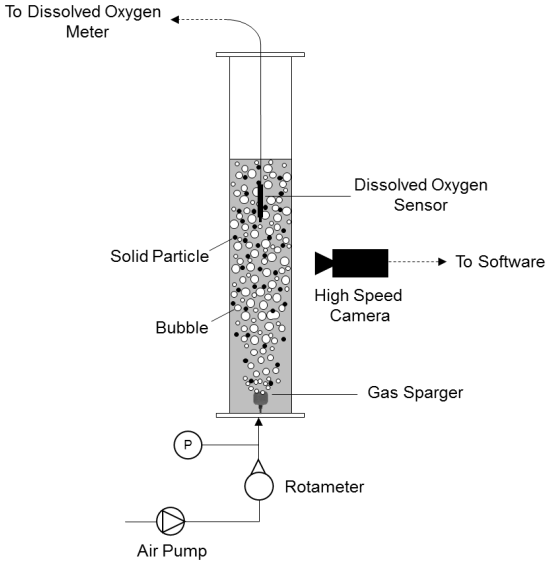

Figure 1 Experimental setup

2.1.2 Solid Particles

The solid particles added to the bubble column were vary in shapes and sizes. From the previous work, it was found that the most appropriate solids adding to the bubble column were the particles with the density close to the liquid phase; otherwise, the solids could accumulate at the bottom of reactor, promoted the coalescence rate of bubbles and diminished the mass transfer rate. Therefore, Polypropylene (PP) solid particles with the density of 946 kg/m^3 were used. The solid shapes including cylinders, spheres, ellipsoids and rings were prepared in order to consider the effect of particle shape on hydrodynamic and mass transfer rate. Photographs of the particles can be seen in Figure 2 and their properties are given in Table 1. These solids were used at solid loading of 2 – 10 % v/v

Table 1 Physical solid particles characteristics.

Shape	Particle equivalent diameter (mm)	Bulk porosity	Shape factor	Terminal velocity[a] (cm/s)
Ring	4.15	0.78	0.35	-1.66
Ellipsoid	3.46	0.40	0.96	-1.98
Sphere	4.00	0.40	1.00	-2.13
Cylinder	3.08	0.43	0.85	-1.97

a) Positive velocity value refers to velocity in the direction of gravity

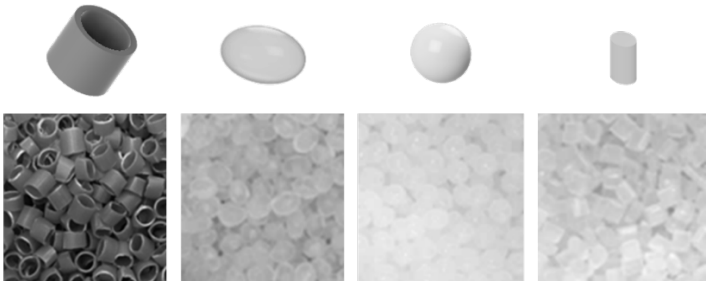

(a) (b) (c) (d)

Figure 2 Solid particles
(a) ring (b) ellipsoid (c) sphere (d) cylinder

2.2 Methods

2.2.1 Determination of overall volumetric mass transfer coefficient (k_La)

The experiments were carried out at 25°C and atmospheric pressure. For each experiment, 150 mg/L of sodium sulfite **(**Na_2SO_3**)** was added into the tap water to reduce the dissolved oxygen in tap water and obtain the oxygen-free liquid. The sulphite concentration was low enough not to cause any changes to the water properties. Afterwards, air was injected upward through a sparger and dissolved oxygen concentrations were measured**.** According to the dynamic method [18], the k_La values could be evaluated from Equation **(**1**).**

$$\frac{dC}{dt} = k_L a.(C^* - C_t) \quad (1)$$

where **C*** and C_t are the saturated concentration of dissolved oxygen in liquid and the concentration of dissolved oxygen measured at time t, respectively; a perfectly mixed reactor is assumed**.** The k_La values can be estimated graphically from the slopes of $\ln(C^* - C_t)$ versus time**.** A CyberScan DO110 dissolved oxygen meter was used to measure dissolved oxygen concentration at the middle of the liquid height level. Noted that the value of C^* in all experiments were equal to 8.25 mg/L according to laboratory temperature and pressure [19].

2.2.2 Determination of bubble diameter (d_B) and bubble rising velocity (U_B)

The bubble sizes were determined at the middle of water height (36 cm above the sparger) with a photographic technique using a high speed camera. A Basler high speed camera (340 images/second) connected to a computer was employed to capture images so that bubble diameter and bubble rising velocity could be determined with the LabVIEW and Image Frame Work programs. Samples of 200-300 bubbles (95% statistical confidence) were randomly chosen from each experiment and their equivalent diameters measured with the Image Frame Work software. The Sauter mean diameter or the surface-to-volume diameter (d_{32}) was used to find the average diameter ($d_{B,avg}$) for each experiment as shown in Equation (2)

$$d_{B,avg} = d_{32} = \frac{\sum_i n_i d_i^3}{\sum_i n_i d_i^2} \quad (2)$$

where n_i is the number of bubbles that have an equivalent diameter d_i. The bubble rising velocity can be estimated from the distance covered by a rising bubble between two frames as in Equation (3).

$$U_B = \frac{\Delta D}{T_{frame}} \quad (3)$$

Where ΔD is the bubble displacement between $t = 0$ and t while T_{frame} is the number of frames/340 second.

2.2.3 Gas holdup (ε_g) determination

The gas holdup is the gas fraction presents in the gas-liquid system or the gas-liquid-solid system (when solids are used). It was calculated from the gas volume (V_g), liquid volume (V_l) and solid volume (V_s) by the Equation (4) [4]:

$$\varepsilon_g = \frac{V_g}{V_g + V_l + V_s} \quad (4)$$

The value of gas hold up could be directly measured experimentally and calculated by comparing the height of the liquid surface levels before (H_B) and after gas flow (H_A) as defined in Equation (5).

$$\varepsilon_g = \frac{(H_A - H_B)}{H_A} \quad (5)$$

2.2.4 Specific interfacial area (a) determination

With the assumption of spherical bubble shape, the gas/liquid interfacial area was estimated from gas holdup, solid holdup and bubble diameter with Equation (6) [6]:

$$a = \frac{6}{d_B} \cdot \frac{\varepsilon_g}{1 - \varepsilon_g - \varepsilon_s} \quad (6)$$

and the solid holdup (ε_s) was calculated by the Equation (7).

$$\varepsilon_s = \frac{V_s}{V_g + V_l + V_s} \quad (7)$$

2.2.5 Determination of specific power consumption (P/V)

The specific power consumption (P/V) is the power consumption per volume of liquid in the reactor (V). The P/V was calculated regarding the total gas pressure drop (ΔP) and its volumetric flow rate (Q) as shown in equation (8) [18].

$$P/V = Q \cdot \Delta P/V \quad (8)$$

3. RESULTS AND DISCUSSION

3.1 Effect of Different Orifice Sizes of Gas Spargers on Gas Phase Hydrodynamics and Mass Transfer

Bubble sizes were observed in the absence of solid phase. Table 2 shows the effects of superficial velocity and orifice size on the average bubble diameter ($d_{B,avg}$) , the gas hold up (ε_g), the interfacial area (a), and the overall mass transfer coefficient (k_La). The table indicates that the average bubble diameter increased with the gas superficial velocity (V_g) and the larger orifice sparger apparently provided larger bubbles. This observation is supported by various works [10,11,18].

Table 2 Hydrodynamic and mass transfer variables at different superficial gas velocity and orifice size

V_G (cm/s)	$d_{B,avg}$ (mm)		ε_g (%)		a (m^{-1})		k_La (s^{-1})	
	SO	LO	SO	LO	SO	LO	SO	LO
0.3	2.73	3.97	1.81	1.07	40.7	16.3	0.008	0.005
0.5	2.93	3.99	2.84	2.11	60.0	32.4	0.012	0.008
0.8	3.04	4.18	3.99	2.99	82.0	44.2	0.015	0.011
1.1	3.47	4.22	4.97	4.13	90.4	61.3	0.016	0.014
1.3	3.62	4.31	6.34	5.25	112.4	77.1	0.017	0.016

a) SO = Small orifice sparger b) LO = Large orifice sparger

For gas hold up, Table 2 indicates two issues regarding the gas hold up. Firstly, the gas hold up increased with the superficial gas velocity due to the higher amounts of bubbles generated at the sparger as higher gas flow increased. Secondly, the small orifice sparger provided higher gas hold up than the large orifice. This was corresponding to the different diameter of bubbles produced by the orifices. According to the smaller size bubbles generated by the small orifice sparger, the small bubbles rise to the liquid surface slower than the large bubbles and eventually stayed in the column longer. As the results, the gas hold up in case of the small orifice sparger was superior to the large one.

Concerning the interfacial area, the larger orifice sparger provided lower specific interfacial areas corresponding to Equation (5) as it provided larger bubble diameters and lower gas holdup while smaller orifice sparger produced small bubbles that yielded higher gas hold up. Moreover, the overall mass transfer coefficient (k_La) for the two spargers were following the same trend as the interfacial area. Since $k_La = k_L \times a$ and k_L values in the operation range increased slightly with bubble size according to the relation found by Sardeing et al. [20]. Thus, the low specific interfacial area was the predominant cause of the lower k_La values.

At this point, it can be understood why spargers with small orifice are commonly used, since they can provide high mass transfer efficiency due to high specific interfacial areas and volumetric mass transfer coefficients. However, using smaller orifices sparger results in higher power consumption [9,18]. The following part will therefore discuss an alternative solution using solid particles to enhance the specific interfacial area.

3.2 Effect of Solid Particles on Gas Phase Bubble Hydrodynamics and Mass Transfer

The gas flow rate providing a superficial velocity of $1.3x10^{-2}$ m/s was selected for further discussion because the highest hydrodynamic properties. This part will mention the results obtained with different spargers and solid particles. It should be noted that the effects of solids on hydrodynamic and mass transfer were in the same tendency throughout the range of gas superficial velocity studied in this work.

3.2.1 Average bubble diameter ($d_{B,avg}$)

Figure 3 shows that the presence of solid reduced the average bubble diameter ($d_{B,avg}$). This effect was less observed in the case of the small orifice sparger (6.5 – 13% change in size) than with the large orifice sparger (16 – 24 % change) since their initial sizes were smaller. However, it should be taken into account that in case of the small orifice sparger, there was a very small portion of large bubbles (larger than 8 mm) presenting in the column; nonetheless, those small amounts didn't affect the average value since the amount of larges bubble was too low.

In addition, adding too high solid loading might have the reverse effect for some types of particles. This can be evidently observed in Figure 3(b) when more than 2%vol of ellipsoid and sphere shapes were presenting in the column.

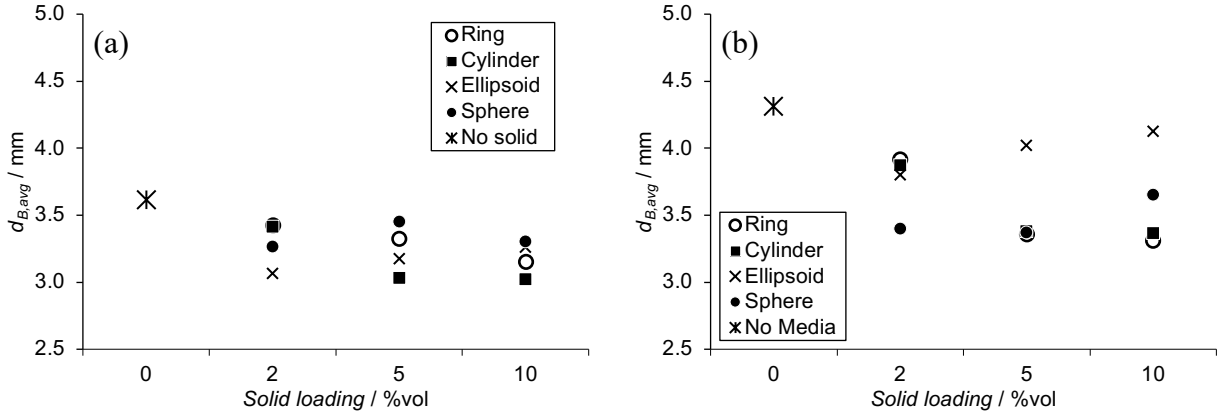

Figure 3 Effect of the solid PP particles on the average bubble diameter at superficial velocity of $1.3x10^{-2}$ m/s using (a) small orifice sparger and (b) large orifice sparger

Normally, the addition of solid phase has three major influences on bubble geometry and flow behaviors: increasing breaking rate, accelerating the coalescence rate, and increasing flow resistance [21–23]. Under different solid concentration and bubble size, the solids would have different effects.

For the case of the large orifice sparger, the addition of solids promoted the breaking rate more than the coalescence; therefore, the average bubble size decreased with presenting of the solids.

However, the addition of solids with the small orifice sparger promoted both bubble breaking rate and bubble coalescence rate because the average bubble diameter was smaller but very large bubbles were seemingly formed. This could be possibly caused by the amount of bubbles generated by the small orifice sparger that was much higher than the large orifice leading to easier chance to promote the coalescence rate [24].

The effect of the solid shape was not clearly observed in the small orifice sparger but it could be clearly seen in the large orifice sparger case, Figure 3(b). Although the average bubble diameter was reduced with the presenting of solids, the addition of ellipsoid and sphere shape particles above 2 %v/v increased the average bubble diameter while the addition of ring and cylinder shapes didn't have the same effect. This possibly caused by the sharp edge effect of the ring and cylinder particles that influenced the bubble breaking rate since the force acting at the edges was be larger than the edgeless particles. The effect was also mentioned by Kim et al. [15,25]. Moreover, it could be seen that the ellipsoid particles reduced the average bubble diameter less than the sphere particles. This implied that the larger particles promoted the bubble breakage rate better than the smaller particles since the sphere particles were larger. Kim et al [15] and Nguyen-tien et al. [16] also mentioned this similar effect.

3.2.2 Bubble rising velocity (U_B)

Figure 4(a) shows the effect of solid loading and shape on the bubble rising velocity in the small orifice sparger's case. In the figure, adding solid particles at any concentration increased the bubble rising velocity which opposited to the results with the large orifice sparger (Figure 4(b)), where the rising velocities were decreased.

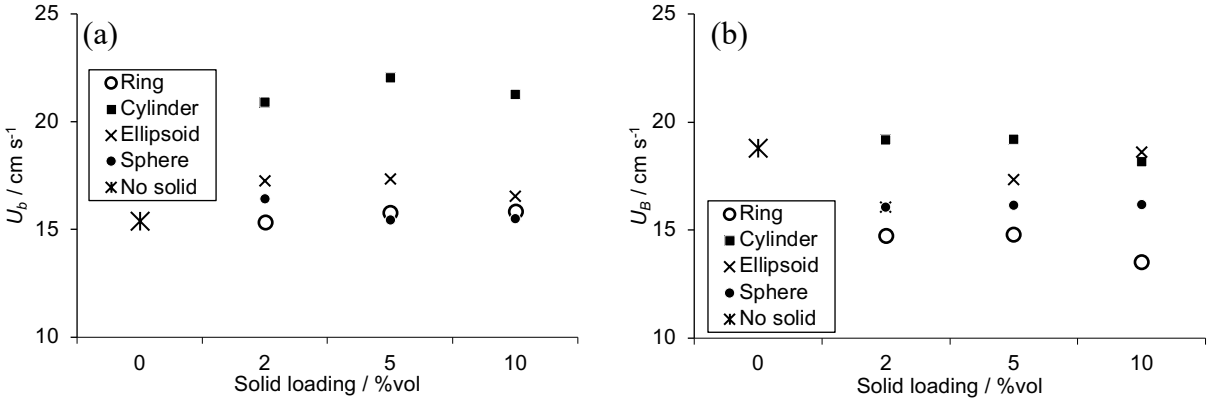

Figure 4 Effect of the solid particles on the bubble rising velocity at superficial velocity $1.3x10^{-2}$ m/s using (a) small orifice sparger (b) large orifice sparger

In case of the small orifice sparger, the increase in U_B was caused by the very large bubbles formed in the column as mentioned in the section 3.2.1. These large bubbles had very high rising velocities and their wakes that formed behind them entrained both solids and other small bubbles upward, causing bubbles to reach the liquid surface faster [26]. Thus, in the case of a small orifice sparger, bubble rising velocities were higher than usual after addition of the solids.

In contrast, Figure 4(b) indicated that the bubble rising velocities were decreased with the presenting of solid concentration in case of the large orifice sparger. Unlike the small orifice sparger, the very large bubbles were not frequently formed. Besides, the presenting of solids may increase the flow resistance that lower the liquid velocity [21] as well as reducing the bubble rising velocity by obstructing them. This effect could be observed especially in case of the ring particles, which had the highest surface area leading to higher drag force.

3.2.3 Gas hold up (ε_g)

As can be observed in Figure 5(a), the gas hold up decreased with the presence of cylinder-shaped particles when a small orifice sparger was used, whereas no obvious effects were noted with other particles types. For a large orifice sparger (Figure 5(b)), the gas holdup was increased with the presence and concentration of ring-shaped particles. Slight effects could be observed in the presence of ellipsoid and spherical particles, while no change with the concentration could be seen for the cylindrical particles. These results were supported by the bubble rising velocities (see Figure 4), where the lower rising velocity resulted in the higher gas hold up in the water because the bubbles rose slower to water surface leading to higher amounts of bubble and gas hold up.

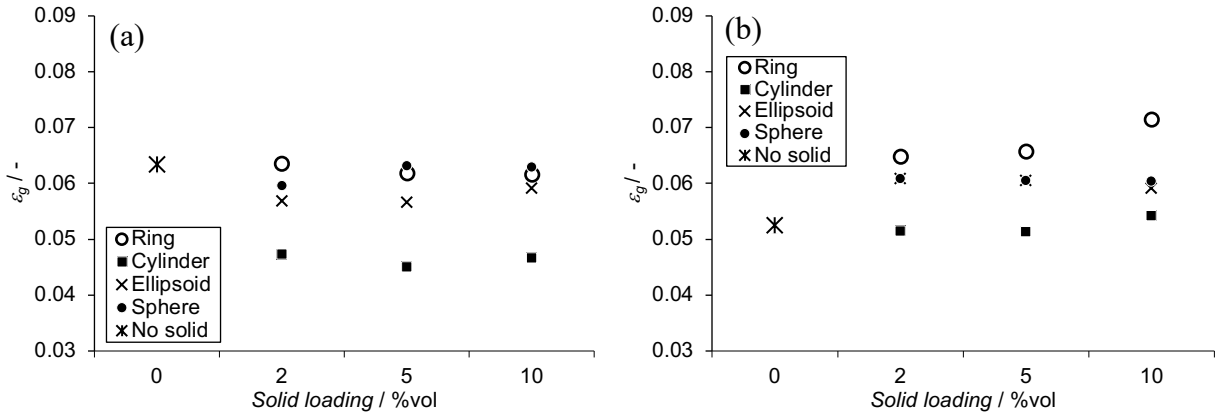

Figure 5 Effect of the solid particles on the gas holdup at superficial velocity of $1.3x10^{-2}$ m/s using (a) small orifice sparger (b) large orifice sparger

3.2.4 Specific interfacial area (a)

The values of bubble diameter and gas hold up were used to calculate the specific interfacial area following the Equation (6). The results are shown in Figure 6(a) and Figure 6(b) for the small and the large orifice sparger respectively.

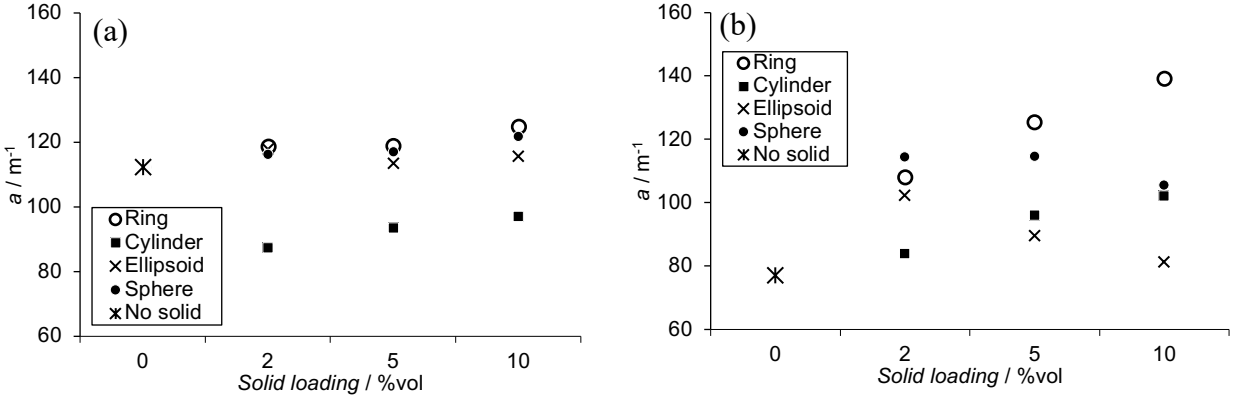

Figure 6 Effect of the solid particles on the specific interfacial area at superficial velocity of $1.3x10^{-2}$ m/s using (a) small orifice sparger (b) large orifice sparger

As shown in Figure 6(a), only cylindrical particles caused the decrease in the specific interfacial areas in case of the small orifice sparger due to the intense decrease of the gas holdup in the small orifice sparger operation. On the other hand, for the large orifice sparger, the specific interfacial areas apparently increased with concentrations for all particles shapes, especially for the ring particles (Figure 6(b)). However, the increasing loading of the ellipsoid and sphere particles above 2%vol deteriorated the specific interfacial area due to the increased bubble diameter (see Figure 3).

3.2.5 Overall volumetric mass transfer coefficient (k_La)

The presence of solid particles in case of the small orifice sparger provided k_La values that slightly lower than the case without solid, as shown in Figure 7(a). On the contrary, particles of any shape, but particularly the ring-shaped particles, could enhance the k_La value due to higher specific interfacial area when the large sparger was applied (Figure 7(b)). The exception of the ellipsoid particles should be noted regarding the k_La values that fell with the solid loading since the specific interfacial area was decreased. The decreasing was not clearly be seen in case of the sphere particles even though their specific interfacial areas were reduced. This was possibly caused by the change of the mass transfer coefficient (k_L) when the solids were presenting [11]. The effect was apparently seen when the small orifice sparger was used as the k_La were reduced despite of their increasing of the interfacial area. This effect should be studied further in order to comprehensively understand the effect of solids on the mass transfer. It should also be taken into account that the ring shape particles were the most appropriate solids that could enhance the k_La by reducing bubble size, bubble rising velocity and increasing gas hold up and interfacial area.

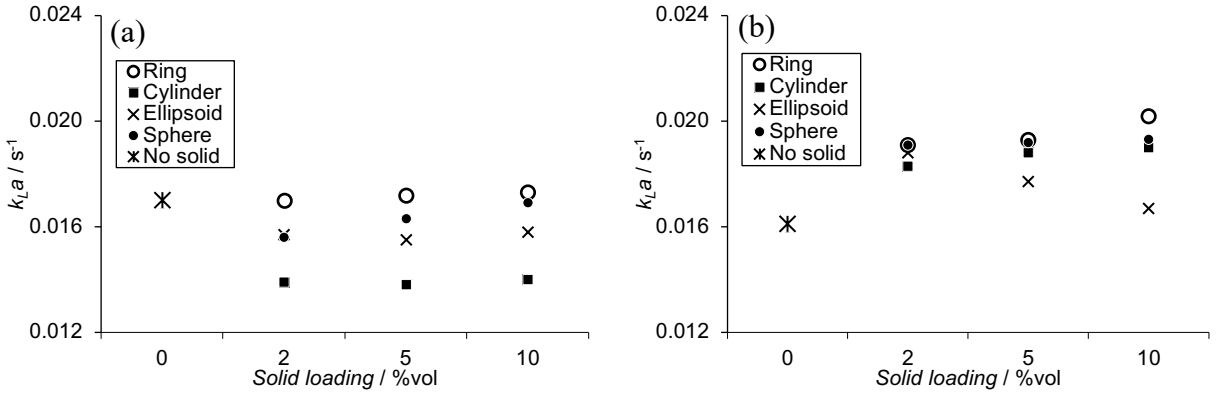

Figure 7 Effect of the solid particles on the overall volumetric mass transfer coefficient at superficial velocity $1.3x10^{-2}$ m/s using (a) small orifice sparger (b) large orifice sparger

In conclusion, the addition of solids particles would have both positive and negative effects. The negative effect could be observed when the small orifice sparger was used. It was presumed that the addition of solids into the small orifice sparger, which produced high amount of bubbles, promoted both breaking and coalescence rate. The large bubbles could be easily formed since there was a lot of bubbles; therefore, the interfacial area and k_La were reduced. The decrease in k_La was likewise observed by the works of Ferreira et al [10] and Mena et al [11] who used the orifice diameter of 0.3 mm and found the negative effect when the solids were presenting in the bubble column.

In contrary, the positive effect could be found when the large orifice sparger was used. The addition of solids phase in this case promoted the breaking rate more than the coalescence rate since the amount of bubble generated at the sparger were not relatively high. This effect was also observed by several works using orifice sparger size around 1 mm [15,16,27].

However, the size of solid particles had to be concerned. Freitas and Teixeira [28] used the solid particles size around 2 mm with the orifice diameter of sparger at 1 mm and found the negative

effect on the mass transfer coefficient that was corresponding to Kim et al [15] who indicated that the solid particles size less than 3 mm would have the negative effect on k_La. In the other hand, Chandraserkaran et al. [12], Sada et al. [13] and Quicker et al [14] used the particles diameter less than 0.1 mm and observed a positive effect on their k_La. Therefore, there was a range of particle size that diminished the k_La and vice versa. It was mentioned by Khare and Josh [29] that the average particle size around 0.1-2 mm could have a negative effect on gas hold up while other size would have the positive effect.

Beside particle size and orifice size, the solid loading concentration could play an important roles on the k_La. In this work, it was found that the increasing in solid loading concentration could have dual effect depending on shape and size of the solid. When the sphere and ellipsoid particles were used, the addition of solids less than 2 % increased the k_La whilst further addition of solids declined the effect. Ozkun et al [17], Albal et al [30] and Mena et al [11] also found the dual effect in their work. This was probably caused by the increase in the coalescence rate when the higher amounts of solids were presenting. However, this observation was not found in case of ring and cylinder shape solid. It was presumed that the sharp edges of the particles were responsible for this phenomena [25].

From the previous explanation, it could be implied that the k_La could be enhanced when the appropriate solid particles were added into the bubble column. In this work, the most appropriate solids were the ring shape particles. The inclusion of the solids could raise the overall mass transfer coefficient without highly additional power consumption. Figure 7 shows the mass transfer coefficient as a function of the specific power consumption of the system.

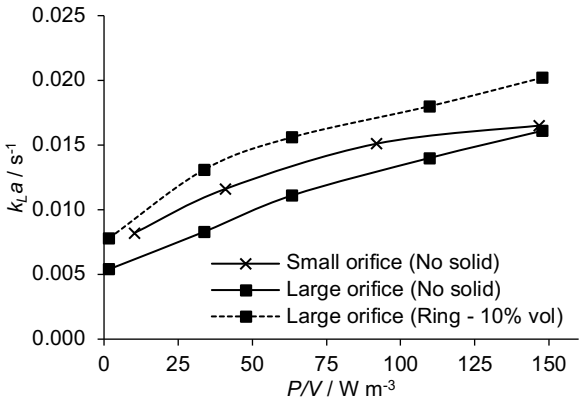

Figure 7 Overall mass transfer coefficient versus the total specific power consumption with different sizes of orifice sparger and with the presenting of ring shape solids

Figure 7 indicates that the k_La were increasing with the specific power consumption regardless of the orifice size. In absence of solids, the k_La of the small orifice sparger was higher than the case of large orifice sparger. However, with the inclusion of ring shape particles with 10% loading in the large orifice sparger bubble column, the k_La increased higher than the k_La of the small orifice case with the same power consumption. This indicated that the presenting of the appropriate solids in the appropriate size of orifice sparger could escalate the k_La without additional power consumption. Therefore, not only higher mass transfer rate was obtained but also lower power required when the appropriate solids were presenting in the system.

In conclusion, the addition of the appropriate solids in the bubble column could rise the mass transfer rate when the bubbles generated with the sparger were not too fine. However, the exact effect of solids on bubble should be investigated in order to comprehensively understand and utilize the knowledge for the design propose [11,17].

4. CONCLUSIONS

The objective of this study was to compare two different rigid-orifice spargers, and four different solid particles that could affect the hydrodynamic and the mass transfer parameters of gas absorption in a bubble column. For this purpose, the spargers were characterized in terms of their sizes while the solid particles were characterized in terms of their shape, physical properties and loading rate (concentration). The results show that:

Bubble diameters increased with orifice sizes. Without the addition of solid, the small orifice sparger was better since it could provide higher specific interfacial area and overall volumetric mass transfer coefficient. However, the power consumption must also be considered.

With addition of solid particles, the average bubble diameters, gas hold up, specific interfacial area, and overall mass transfer coefficient could be positively or negatively changed depended on solid characteristics and sparger orifice size.

The positive effect was apparently observed when the large orifice sparger was applied. The addition of solids increased the bubble breaking rate, reduced the average bubble diameter, and consecutively increased gas hold up, interfacial area, and the overall mass transfer coefficient (k_La).

The negative effect could be encountered when the small orifice sparger was used. In this case, the inclusion of solids rose both bubble breaking rate and coalescence rate since the small orifice sparger produced high amounts of bubbles leading them to coalesce into larger bubble easily. The large bubble formed in the column rose upward rapidly and entrained other bubbles upward faster via their wakes. This eventually reduced the gas hold up and negatively affected the k_La.

The shape, size and loading rate also had the effects on both hydrodynamic and mass transfer. It was found that (1) the solids with sharp edges had better potential to rise the bubble breaking rate, (2) the larger solid particles improved the k_La superior to the small ones, and (3) the ring shape solids were found to be the optimal particles thanks to its hollow and surface area that could reduce the liquid velocity circulating in the column with their drag force resulting in higher gas hold up and eventually the k_La. With this particles, a better mass transfer operation could occur in the bubble column, even with the same gas throughput and the same power consumption.

In the future, further studies will be needed for a thorough investigation and better understanding concerning the presence of particles, especially the effect of the different particles characteristics on the measured mass transfer.

NOMENCLATURE

Alphabetical Symbols

a	specific interfacial area (m^{-1})
C	oxygen concentration at time t (mg/L)
C^*	saturated oxygen concentration (mg/L)
d_B	bubble diameter (μm)
d_{32}	Sauter mean diameter (μm)
d_{avg}	average bubble diameter (μm)
d_i	bubble diameter number i (μm)
Δd	different in liquid level before and after gas throughput (m)
H_A	level of liquid after gas throughput (m)
H_B	level of liquid before gas throughput (m)
k_L	mass transfer coefficient (m/s)
n_i	bubble number i (-)
P	power consumption (W)
U_B	bubble rising velocity (cm/s)
V	reactor volume (m^3)
V_g	gas volume in reactor (m^3)
V_L	liquid volume in reactor (m^3)

V_s solid volume in reactor (m^3)
t corresponding time (s)
t_c contact time (s)
t_{frame} time between each frame of camera (s)

Greek Letter Symbols

ε_g gas hold up or gas fraction (-)
ε_L liquid hold up or liquid fraction (-)
ε_s solid hold up of solid fraction (-)

ACKNOWLEDGEMENT

The authors acknowledge the financial support given by "The 100th Year Anniversary Chulalongkorn University Fund for Doctoral Scholarship", "The 90th Anniversary Chulalongkorn University Fund (Ratchadaphiseksomphot Endowment Fund)" and "Ratchadapisek Sompoch Endowment Fund (2016) CU-59-052-CC" from Chulalongkorn university.

REFERENCES

[1] N. Kantarci, F. Borak, K.O. Ulgen, Bubble column reactors, Process Biochem. 40 (2005) 2263–2283. doi:10.1016/j.procbio.2004.10.004.
[2] A. García-Abuín, D. Gómez-Díaz, M. Losada, J.M. Navaza, Bubble column gas–liquid interfacial area in a polymer+surfactant+water system, Chem. Eng. Sci. 75 (2012) 334–341. doi:10.1016/j.ces.2012.03.054.
[3] X. Jia, W. Hu, X. Yuan, K. Yu, Effect of surfactant type on interfacial area and liquid mass transfer for CO2 absorption in a bubble column, Chin. J. Chem. Eng. 23 (2015) 476–481. doi:10.1016/j.cjche.2014.11.027.
[4] G. Hebrard, J. Zeng, K. Loubiere, Effect of surfactants on liquid side mass transfer coefficients: A new insight, Chem. Eng. J. 148 (2009) 132–138. doi:10.1016/j.cej.2008.08.027.
[5] L. Luo, F. Liu, Y. Xu, J. Yuan, Hydrodynamics and mass transfer characteristics in an internal loop airlift reactor with different spargers, Chem. Eng. J. 175 (2011) 494–504. doi:10.1016/j.cej.2011.09.078.
[6] G. Hébrard, D. Bastoul, M. Roustan, Influence of the Gas Sparger on the Hydrodynamic Behaviour of Bubble Columns, Chem. Eng. Res. Des. 74 (1996) 406–414.
[7] S. Moustiri, G. Hebrard, M. Roustan, Effect of a new high porosity packing on hydrodynamics of bubble columns, Chem. Eng. Process. Process Intensif. 41 (2002) 419–426. doi:10.1016/S0255-2701(01)00162-3.
[8] B. Bhatia, K.D.P. Nigam, D. Auban, G. Hebrard, Effect of a new high porosity packing on hydrodynamics and mass transfer in bubble columns, Chem. Eng. Process. Process Intensif. 43 (2004) 1371–1380. doi:10.1016/j.cep.2003.10.009.
[9] J.G.G. Maldonado, D. Bastoul, S. Baig, M. Roustan, G. Hébrard, Effect of solid characteristics on hydrodynamic and mass transfer in a fixed bed reactor operating in co-current gas–liquid up flow, Chem. Eng. Process. Process Intensif. 47 (2008) 1190–1200. doi:10.1016/j.cep.2007.02.013.
[10] A. Ferreira, C. Ferreira, J.A. Teixeira, F. Rocha, Temperature and solid properties effects on gas–liquid mass transfer, Chem. Eng. J. 162 (2010) 743–752. doi:10.1016/j.cej.2010.05.064.
[11] P. Mena, A. Ferreira, J.A. Teixeira, F. Rocha, Effect of some solid properties on gas–liquid mass transfer in a bubble column, Chem. Eng. Process. Process Intensif. 50 (2011) 181–188. doi:10.1016/j.cep.2010.12.013.

[12] K. Chandraserkaran, M.M. Sharma, Absorption of oxygen in aqueous solutions of sodium sulfide in the presence of activated carbon as catalyst, Chem. Eng. Sci. 32 (1977) 669–671. doi:10.1016/0009-2509(77)80233-9.
[13] E. Sada, H. Kumazawa, C. Lee, N. Fujiwara, Gas-liquid mass transfer characteristics in a bubble column with suspended sparingly soluble fine particles, Ind. Eng. Chem. Process Des. Dev. 24 (1985) 255–261. doi:10.1021/i200029a006.
[14] G. Quicker, A. Schumpe, W.-D. Deckwer, Gas-liquid interfacial areas in a bubble column with suspended solids, Chem. Eng. Sci. 39 (1984) 179–183. doi:10.1016/0009-2509(84)80150-5.
[15] J.O. Kim, S.D. Kim, Gas-Liquid mass transfer in a three-phase fluidized bed with floating bubble breakers, Can. J. Chem. Eng. 68 (1990) 368–375. doi:10.1002/cjce.5450680303.
[16] K. Nguyen-Tien, A.N. Patwari, A. Schumpe, W.-D. Deckwer, Gas-liquid mass transfer in fluidized particle beds, AIChE J. 31 (1985) 194–201. doi:10.1002/aic.690310204.
[17] O. Ozkan, A. Calimli, R. Berber, H. Oguz, Effect of inert solid particles at low concentrations on gas–liquid mass transfer in mechanically agitated reactors, Chem. Eng. Sci. 55 (2000) 2737–2740. doi:10.1016/S0009-2509(99)00532-1.
[18] M. Bouaifi, G. Hebrard, D. Bastoul, M. Roustan, A comparative study of gas hold-up, bubble size, interfacial area and mass transfer coefficients in stirred gas–liquid reactors and bubble columns, Chem. Eng. Process. Process Intensif. 40 (2001) 97–111. doi:10.1016/S0255-2701(00)00129-X.
[19] H.E. Garcia, L.I. Gordon, Oxygen solubility in seawater: Better fitting equations, Limnol. Oceanogr. 37 (1992) 1307–1312. doi:10.4319/lo.1992.37.6.1307.
[20] R. Sardeing, P. Painmanakul, G. Hébrard, Effect of surfactants on liquid-side mass transfer coefficients in gas–liquid systems: A first step to modeling, Chem. Eng. Sci. 61 (2006) 6249–6260. doi:10.1016/j.ces.2006.05.051.
[21] T. Zhang, J. Wang, Z. Luo, Y. Jin, Multiphase flow characteristics of a novel internal-loop airlift reactor, Chem. Eng. J. 109 (2005) 115–122. doi:10.1016/j.cej.2005.03.014.
[22] A.G. Livingston, S.F. Zhang, Hydrodynamic behaviour of three-phase (gas—liquid—solid) airlift reactors, Chem. Eng. Sci. 48 (1993) 1641–1654. doi:10.1016/0009-2509(93)80124-9.
[23] J.W.A. De Swart, R.E. van Vliet, R. Krishna, Size, structure and dynamics of “large” bubbles in a two-dimensional slurry bubble column, Chem. Eng. Sci. 51 (1996) 4619–4629. doi:10.1016/0009-2509(96)00265-5.
[24] M.J. Prince, H.W. Blanch, Bubble coalescence and break-up in air-sparged bubble columns, AIChE J. 36 (1990) 1485–1499. doi:10.1002/aic.690361004.
[25] S.-D. Kim, H.-S. Jang, Hydrodynamics and Bubble Breakage in Three Phase Fluidized Beds, Korean Chem. Eng. Res. 17 (1979) 407–407.
[26] Y. Li, J. Zhang, L.-S. Fan, Numerical simulation of gas–liquid–solid fluidization systems using a combined CFD-VOF-DPM method: bubble wake behavior, Chem. Eng. Sci. 54 (1999) 5101–5107. doi:10.1016/S0009-2509(99)00263-8.
[27] V.R. Dhanuka, J.B. Stepanek, Simultaneous measurement of interfacial area and mass transfer coefficient in three-phase fluidized beds, AIChE J. 26 (1980) 1029–1038. doi:10.1002/aic.690260619.
[28] C. Freitas, J.A. Teixeira, Oxygen mass transfer in a high solids loading three-phase internal-loop airlift reactor, Chem. Eng. J. 84 (2001) 57–61. doi:10.1016/S1385-8947(00)00274-6.
[29] A.S. Khare, J.B. Joshi, Effect of fine particles on gas hold-up in three-phase sparged reactors, Chem. Eng. J. 44 (1990) 11–25. doi:10.1016/0300-9467(90)80050-M.
[30] R.S. Albal, Y.T. Shah, A. Schumpe, N.L. Carr, Mass transfer in multiphase agitated contactors, Chem. Eng. J. 27 (1983) 61–80. doi:10.1016/0300-9467(83)80053-7.